Journal Pre-proofs

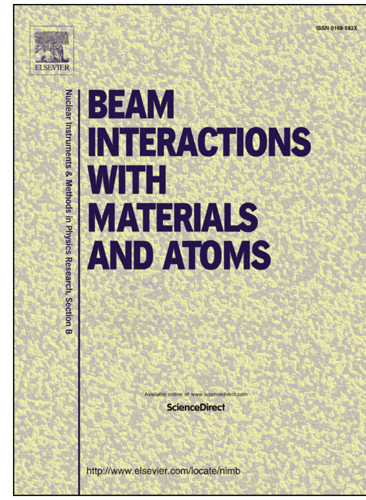

Grazing-incidence transmission SAXS investigation of conical etched ion tracks in SiO_2

A. Hadley, C. Notthoff, P. Mota-Santiago, N. Kirby, P. Kluth

PII: S0168-583X(19)30815-8
DOI: https://doi.org/10.1016/j.nimb.2019.12.006
Reference: NIMB 63981

To appear in: *Nucl. Instr. and Meth. in Phys. Res. B*

Received Date: 23 October 2019
Revised Date: 9 December 2019
Accepted Date: 10 December 2019

Please cite this article as: A. Hadley, C. Notthoff, P. Mota-Santiago, N. Kirby, P. Kluth, Grazing-incidence transmission SAXS investigation of conical etched ion tracks in SiO_2, *Nucl. Instr. and Meth. in Phys. Res. B* (2019), doi: https://doi.org/10.1016/j.nimb.2019.12.006

REY-20
ASTANA 2019

MANUSCRIPT LENGTH ESTIMATE

Beam Interactions with Materials and Atoms
Nuclear Instruments and Methods in Physics Research, Section B.

Title of Paper: GRAZING-INCIDENCE TRANSMISSION SAXS INVESTIGATION OF CONICAL ETCHED ION TRACKS IN SiO_2

Corresponding Author :Andrea Hadley

Manuscript Length Estimation Table

Number of characters[1] (using "character count")	**22151**	**= A**
Number of 1-column tables or figures[2]	**7**	**= B**
Number of 2-column tables or figures[2]		**= C**

Estimated number of printed pages	**= (A + 1300B + 5000C)/8500**	**3.7**

[1] Including title, abstract, captions and references, including spaces.
[2] Each independent figure including Fig.a, Fig.b, Fig.c, etc. must be counted separately.

GRAZING-INCIDENCE TRANSMISSION SAXS INVESTIGATION OF CONICAL ETCHED ION TRACKS IN SiO_2

A. Hadley,[a] C. Notthoff,[a] P. Mota-Santiago,[a] N. Kirby,[b] and P. Kluth[a]

[a] Department of Electronic Materials Engineering, Research School of Physics, Australian National University, Canberra, Australia.

[b] Australian Synchrotron, ANSTO; 800 Blackburn Rd, Clayton, Australia,

ABSTRACT

We present results of a systematic study of the morphology of etched ion tracks in amorphous SiO_2 using a combination of small angle x-ray scattering (SAXS) and scanning electron microscopy. We focus on the analysis of SAXS data obtained in grazing incidence (GISAXS) configuration from conical etched channels with a base radius of less than 50 nm. Swift heavy ion irradiation of 2 μm thick thermally grown SiO_2 layers with 185 MeV Au ions was conducted at the ANU Heavy Ion Accelerator Facility in Canberra, Australia. Low irradiation fluences of 10^9 ions per cm^2 were chosen to minimize overlap of the etched structures. Irradiated samples were etched in aqueous hydrofluoric acid (HF) with concentrations of 5 %, for etching times between 30 and 90 seconds. In grazing incidence configuration, we obtain good data quality from the very small cones, since the x-ray beam interacts with a greater proportion of the sample at the very low incidence angle compared with normal transmission mode.

The increased susceptibility to chemical etching of regions of solids exposed to irradiation by high energy heavy ions was first recognised by Young [1]. Damage from recoiling fission fragments in ionic crystals could be etched and rendered observable by optical microscopy. The etched track density could then be correlated with that of the fission fragments the material was exposed to. As heavy ion accelerators became available in the 1960s and 70s it was soon discovered that etched ion tracks could be made in a variety of materials in a controlled way [2, 3]. Recently nanoscale pores generated by the ion track etching technique have been used for bio-sensing applications, where the tip of the pore is able to detect the passage of a single molecule [4-6]. Pores in materials such as SiO_2 are very interesting for sensing applications because they are mechanically and thermally robust, providing the opportunity for direct integration with silicon technology [7].

Artificial membranes with nano-sized pores fabricated in dielectric materials have promising applications in biological and electrical sensing, filtration, and for novel electronic devices, due to their robustness and compatibility with standard semiconductor processing. Using the ion track etching technique, it is possible to produce conically shaped pores with tip openings as small as just a few nanometres, but the size of the openings can be very difficult to measure directly [8, 9]. To realise specific applications such as nanopore sensors, it is necessary to be able to accurately characterise the ion track etching behaviour. To address this we have conducted a systematic study of the etching behaviour of ion tracks in SiO_2 [10]. Using small angle x-ray scattering supported by SEM imaging, we were able to accurately measure the track etch rates in both the lateral and radial directions, as well as the cone opening angles. In the previous study accurate characterisation was limited to cone radii at the base larger than 25 nm because of the very small scattering volume of the smaller pores. In this paper, we extend the results reported in [10] by using transmission SAXS in grazing incidence configuration (GTSAXS). In this configuration, it was possible to accurately measure cones with base radii smaller than around 25 nm because the x-ray beam interacts with significantly more conical pores due to the grazing angle. The increased number of scattering objects leads to a significantly improved signal that scattering of the x-ray beam from the substrate, further improving the signal to noise ratio of the detected scattering pattern.

EXPERIMENTAL

Sample preparation

Samples were prepared from commercially obtained 2 μm thick thermally grown amorphous SiO_2 (a-SiO_2) layers on Si wafer substrates. They were irradiated at the ANU Heavy Ion Accelerator Facility with 185 MeV Au ions at room temperature normal to the sample surface to a fluence of $1x10^9$ ions cm^{-2}. Samples were subsequently chemically etched for 30, 60 and 90 s at room temperature in a dilute (5% by volume) aqueous HF solution, yielding parallel, almost monodisperse conical etch pits in the SiO_2 layer. The general conical shape of the etched pores was confirmed by SEM as shown in Fig. 1.

GTSAXS measurement set-up

GTSAXS measurements were conducted at the SAXS/WAXS beam line of the Australian Synchrotron. Samples were mounted horizontally on a three-axis goniometer. In normal transmission SAXS configuration the conical etched ion tracks are aligned coaxially with the x-ray beam. In grazing incidence configuration, the conical etched tracks are oriented with their axes at approximately 90° to the x-ray beam. Figure 2 (adapted from [11]) shows the position of the sample with respect to the x-ray beam, with the incident beam shown as a red arrow. The transmitted part of the scattered x-ray beam which is utilised in this work is shown in pink. The part of the scattered beam indicated in green is the normal grazing incidence scattered signal. Measurements were performed with an x-ray photon energy of 11 keV with a sample to detector distance of 1240 mm. The incidence angle α was scanned from 0° to 2° in increments of 0.1° to ensure the orientation of the sample was optimised.

Transmission mode SAXS has successfully been used to characterise cylindrical ion tracks in SiO_2 [12, 13], and to characterise etched ion tracks in a variety of materials [10, 14-16]. The scattering amplitude recorded by the detector is related to the three-dimensional variation in the electron density of the sample. The general expression for the scattering amplitude is

$$f(\mathbf{q}) = \iiint \rho(\mathbf{r}) exp^{-i\,(\mathbf{q}.\mathbf{r})}\, d^3r \qquad (1)$$

where $\rho(\mathbf{r})$ is the three-dimensional variation in electron density in the material. For etched ion tracks we assume a density profile in the radial direction with an abrupt transition from the etched region to the remaining material. Provided the density inside the etched track is constant, the scattering amplitude for cylindrical etched ion tracks may be given as

$$f(q_r) = \frac{2\pi\, L\, R\, \Delta\rho}{q_r} J_1\,(Rq_r) \qquad (2)$$

[12], where $\triangle\rho$ is the density contrast between the etched region of the track and the remaining unetched material, *L* is the length of the etched track, *R* is the track radius, J_1 is the Bessel function of the first order and the scattering amplitude, and $q_r = \sqrt{{q_x}^2 + {q_y}^2}$. The scattering amplitude for a cylinder may be used as an approximation for that of conical etched tracks provided they are small and well separated [10]. The reference frame we choose is fixed to the cone axis (*z* direction), and in normal transmission SAXS mode the etched ion tracks are coaxially aligned with the incident x-ray beam.

When the samples are mounted in GTSAXS configuration, the axes of the etched tracks are tilted by approximately 90° with respect to the x-ray beam. Under these conditions the half cone opening angle β may be directly obtained from the angle between features in the scattering pattern as shown in Fig. 3, and discussed in reference [17]. β is related to the height of the cone, H, and the base radius of the cone R_0, by equation 3. For the results presented in this paper, the radius values were obtained by analyzing the intensities using equation 2.

$$R_0 = H \tan\beta \qquad (3)$$

Figure 1(a) and (b) are SEM images of conical etch pits in a layer of a-SiO_2 which have been cleaved to show the cones in cross-section. This sample was etched in 5% HF for 90 seconds, and the conical shape of the etch pits can clearly be seen. In Fig. 1 (a) the sample is tilted with respect to the electron beam by 45° and etched conical pits which are randomly distributed and well separated can be seen on the surface. At the bottom right of the image circled in white, a conical etched pit can be seen in cross section on the cleaved edge. In Fig. 1(b) the same sample is oriented with the cleaved edge at approximately 90° with respect to the electron beam. At the centre of the image, circled in white, a close-up view of the cross section of a conical etch pit can be seen. While these images show directly that the shape of the etch pits is conical, they highlight how small they are. The vertical lines evident in the SiO_2 layer are an artefact of the sample preparation and are most likely not due to ion track damage since they are not in line with the etched ion tracks. It is very difficult to obtain accurate measurements from the SEM cross section due to poor statistics, charging of the insulating sample, and artefacts resulting from sample cleaving. This is particularly relevant for the small cones in this study.

An example of grazing incidence small angle x-ray scattering (GISAXS) data showing transmission scattering from the same sample shown in Fig. 1 (a) and (b) is shown in Fig. 3. The dotted line across the image represents the horizon between grazing incidence scattering above the line, and transmission scattering below the line. The large blue rectangular shaped object in the centre of the image is the shadow of the beam stop which protects the detector from the intense reflected x-ray beam. Two pairs of streaks are clearly resolved in the transmission part of the image. The inset in Fig. 3 is the normal transmission mode scattering pattern recorded for the same sample. In comparison to the GTSAXS data, the scattering in normal transmission mode is very weak and no streaks due to scattering from the conical pores could be seen above the background noise.

1-D data fits obtained using equation 2 for three samples etched for 30, 60 and 90 seconds in 5% HF are shown in Fig. 4 and the results are summarised in Table 1. The results of the data fits are plotted in Fig. 5 (blue data points). The data points shown in red were previously measured by transmission previously obtained results for the 5% HF etching series to very small conical etch pits with radii as small as 14.6 ± 0.5 nm, for the shortest etching time of 30 s.

Results from analysis of the GTSAXS data continue the linear trend exhibited by the previously published transmission mode SAXS results, as can be seen in Figs. 5 (a) and (b). The etch rates in the axial (υ_a) and radial (υ_r) directions may be deduced from the slope of the fits plotted in Figs. 5 (a) and (b) respectively. For the etching time series results shown in Fig. 5, υ_a = 97.8 ± 3.5 nm/min and υ_r = 17.8 ± 0.8 nm/min, where the uncertainties are derived from the fit. In the radial direction, the y intercept is 5.7 ± 1.8 nm, which compares well with the unetched ion track radius for 185 MeV Au ions of 54 ± 1 Å in a-SiO_2 published by Kluth *et al.* [12]. The continued linear trend in the radius values as the etch pits get smaller is not necessarily expected since these dimensions are approaching the damaged region of the ion tracks. In this region the etching behaviour may no longer be linear as observed, with faster etching occurring close to the ion track in the radial direction.

The cone opening angles were measured directly form the scattering images as indicated by the angle ϕ shown in Fig. 3. The measured results are plotted in Fig. 5 (c), along with cone opening angles previously measured by transmission SAXS (red data points). There is little variation in the measured cone opening angles with etching time. The larger uncertainty for the shortest etching time is due to the very weak scattering making it more difficult to accurately measure the angle between the streaks.

For the study of etched ion tracks it is usual to choose an irradiation fluence of around 1x10^8 ions cm^{-2} to ensure minimal overlap of the etched pores [18, 19]. Samples in this work were irradiated to a fluence of 1 x 10^9 ions cm^{-2}. However, we found that there was not sufficient scattering volume to produce a scattering signal with features that could be analysed when the measurements were made in normal transmission mode, because the signal to noise ratio was too low. The scattering volume is proportional to the number of scattering objects in the path of the x-ray beam. For an x-ray beam spot size of approximately 100 (width) x 25 (height) μm^2 and an ion fluence of 1 x 10^9 ions cm^{-2}, the number of pores covered by the footprint of the x-ray beam in normal transmission mode is approximately 2.5

x 10^2. In GISAXS configuration if the sample is inclined by 4° the footprint of the x-ray beam will increase to 100 x 1420 μm^2. The scattering volume is proportional to the number of pores illuminated by the x-ray beam and grazing incidence configuration effectively increases the scattering volume by at least 60 times. A further advantage of the GTSAXS technique is the ability to reduce or eliminate noise from scattering from the sample substrate. Due to the grazing angle the x-ray beam does not enter the substrate, resulting in much less background noise. Increasing the integration time in normal transmission SAXS mode is possible but the longer exposure times also lead to increased background scattering from the substrate making the scattering signal from the small cones difficult to resolve.

Despite the advantages of the GTSAXS technique for measurements of small cones, we are not proposing it as a substitute for more routine measurements of larger cones because the experimental set-up is more complex and measurements are more time consuming. It is also not a good technique for measurements of very high aspect ratio conical etched tracks because the grazing angle may prevent the x-ray beam from interacting with the entire length of the etched tracks.

In this paper we have demonstrated the use of GTSAXS for the accurate measurement of very small conical etch pits in SiO_2. Using GTSAXS we were able to extend the range of the etched ion tracks we could measure by transmission mode SAXS to radii values as small as 14 nm. A further benefit of using the GTSAXS technique is that we can obtain the cone opening angle directly from the scattering image. Also, the analysis techniques used to extract the cone radius from the data are the same as those already established for analysis of ion tracks using normal transmission mode SAXS.

ACKNOWLEDGEMENTS

Part of the research was undertaken at the SAXS/WAXS beamline at the Australian Synchrotron, part of ANSTO, and we thank the beamline scientists for their technical assistance. Irradiation was conducted at the ANU Heavy Ion Accelerator Facility (HIAF), and we also thank the ANU HIAF staff for their technical assistance. Operations of the ANU HIAF is financially supported by the National Collaborative Research Infrastructure Strategy (NCRIS) HIA capability. This research was supported by an Australian Government Research Training Program (RTP) Scholarship. The authors also acknowledge financial support from the Australian Research Council (ARC) and the German Research Foundation (DFG).

1. Young, D.A., *Etching of radiation damage in Lithium Fluoride.* Nature, 1958(4632): p. 375-377.
2. Fischer, B.E.S., R., *Ion Tracks and Microstructure Technology.* International Journal of Radiation Applications and Instrumentation, 1988. **15**(Part D): p. 75-79.
3. Trautmann, C., *Micro- and nano-engineering with ion tracks: Ion beams in nanoscience and technology*. Topics Applied Physics, ed. R. Hellborg, Whitlow, H., Zhang Y. Vol. 110. 2009: Springer-Verlag.
4. Guo, W., J.M. Xue, W.M. Zhang, X.Q. Zou, and Y.G. Wang, *Electrolytic conduction properties of single conical nanopores.* Radiation Measurements, 2008. **43, Supplement 1**(0): p. S623-S626.
5. Pérez-Mitta, G., A.G. Albesa, C. Trautmann, M.E. Toimil-Molares, and O. Azzaroni, *Bioinspired integrated nanosystems based on solid-state nanopores: "iontronic" transduction of biological, chemical and physical stimuli.* Chemical Science, 2017. **8**(2): p. 890-913.
6. Pérez-Mitta, G., A.S. Peinetti, M.L. Cortez, M.E. Toimil-Molares, C. Trautmann, and O. Azzaroni, *Highly Sensitive Biosensing with Solid-State Nanopores Displaying Enzymatically Reconfigurable Rectification Properties.* Nano Letters, 2018. **18**(5): p. 3303-3310.
7. Uddin, A., S. Yemenicioglu, C.H. Chen, E. Corigliano, K. Milaninia, and L. Theogarajan, *Integration of solid-state nanopores in a 0.5 μm CMOS foundry process.* Nanotechnology, 2013. **24**(15): p. 155501.
8. Vlassiouk, I., P.Y. Apel, S.N. Dmitriev, K. Healy, and Z.S. Siwy, *Versatile ultrathin nanoporous silicon nitride membranes.* Proc Natl Acad Sci U S A, 2009. **106**(50): p. 21039-44.
9. Siwy, Z.S., *Ion-Current Rectification in Nanopores and Nanotubes with Broken Symmetry.* Advanced Functional Materials, 2006. **16**(6): p. 735-746.
10. Hadley, A., C. Notthoff, P. Mota-Santiago, U.H. Hossain, N. Kirby, M.E. Toimil-Molares, C. Trautmann, and P. Kluth, *Etched ion tracks in SiO_2 characterised by small angle x-ray scattering: influence of ion energy and etching conditions.* Nanotechnology, 2019.
11. Lu, X., K.G. Yager, D. Johnston, C.T. Black, and B.M. Ocko, *Grazing-incidence transmission X-ray scattering: surface scattering in the Born approximation.* Journal of Applied Crystallography, 2013. **46**(1): p. 165-172.
12. Kluth, P., C. Schnohr, O. Pakarinen, F. Djurabekova, D. Sprouster, R. Giulian, M. Ridgway, A. Byrne, C. Trautmann, D. Cookson, K. Nordlund, and M. Toulemonde, *Fine Structure in Swift Heavy Ion Tracks in Amorphous SiO_2.* Physical Review Letters, 2008. **101**(17).
13. Mota-Santiago, P., H. Vazquez, T. Bierschenk, F. Kremer, A. Nadzri, D. Schauries, F. Djurabekova, K. Nordlund, C. Trautmann, S. Mudie, M.C. Ridgway, and P. Kluth, *Nanoscale density variations induced by high energy heavy ions in amorphous silicon nitride and silicon dioxide.* Nanotechnology, 2018. **29**(14): p. 144004.
14. Hossain, U.H., M. Rodriguez, D. Schauries, A. Hadley, M. Schleberger, C. Trautmann, S. Mudie, and P. Kluth, *SAXS investigation of un-etched and etched ion tracks in polycarbonate.* Nuclear Instruments and Methods in Physics Research, 2017. **409**.
15. Kuttich, B., M. Engel, C. Trautmann, and B. Stühn, *Tailored nanochannels of nearly cylindrical geometry analysed by small angle X-ray scattering.* Applied Physics A, 2013. **114**(2): p. 387-392.
16. Nadzri, A., D. Schauries, B. Afra, M. Rodriguez, P. Mota, S. Muradoglu, A. Hawley, and P. Kluth, *SAXS study on the morphology of etched and un-etched ion tracks in apatite.* Chemical Geology, 2016. **91**: p. 00009.
17. Hadley, A., C. Notthoff, P. Mota-Santiago, S. Dutt, S. Mudie, M.A. Carrillo-Solano, M.E. Toimil-Molares, C. Trautmann, and P. Kluth, *Analysis of nanometre sized aligned conical pores using SAXS*. 2019.

Toulemonde, and R.M. Papaléo, *Nanoporous SiO_2/Si thin layers produced by ion track etching: Dependence on the ion energy and criterion for etchability.* Journal of Applied Physics, 2008. **104**(2): p. 024307.

19. Milanez Silva, C., P. Varisco, A. Moehlecke, P.P. Fichtner, R.M. Papaléo, and J. Eriksson, *Processing of nano-holes and pores on SiO_2 thin films by MeV heavy ions.* Nuclear Instruments and Methods in Physics Research Section B: Beam Interactions with Materials and Atoms, 2003. **206**: p. 486-489.

and etched in 5% HF for the etching times indicated.

TABLES

Table 1.

Sample etching time (s)	R_0 (nm)	β (°)	H (nm)
30	14.6 ± 0.5	12.5 ± 2.0	76 ± 5
60	22.7 ± 2.0	12.0 ± 1.0	125 ± 5
90	35.7 ± 2.0	12.5 ± 1.0	191 ± 5

FIGURE 1. SEM micrographs of conical etched ion tracks in a 2 μm SiO_2 layer irradiated with 185 MeV Au ions and etched in 5% HF for 90 seconds: (a) 35000 X magnification, inclined at 45° with respect to the electron beam, (b) 50000 X magnification with the sample tilted to 90° with respect to the electron beam.

FIGURE 2. Schematic of GTSAXS configuration (after [11], reproduced with permission of the International Union of Crystallography).

FIGURE 3. Example of GISAXS data for a sample irradiated with 185 MeV Au ions and etched for 90 s in 5% HF, showing the transmitted GTSAXS data below the dotted horizon line, and the normal GISAXS data above the horizon line. The inset is the transmission configuration SAXS data for the same sample tilted at 25° to the incident x-ray beam.

FIGURE 4. Fits of GTSAXS data obtained using equation 2. The data have been off-set on the intensity axis for clarity.

FIGURE 5. Parameters extracted by GTSAXS (blue) together with those extracted by transmission mode SAXS (red data points previously published in [10]) for an etching time series for samples irradiated with 185 MeV Au ions and etched with 5% HF. (a) Etch depth vs etching time, (b) Radius vs etching time and (c) Cone opening angle vs etching time. The slope of the linear fits in (a) and (b) give the axial, ν_a, and radial, ν_r, etch rates. The black solid line plotted in (c) is a guide to the eye.

FIGURES

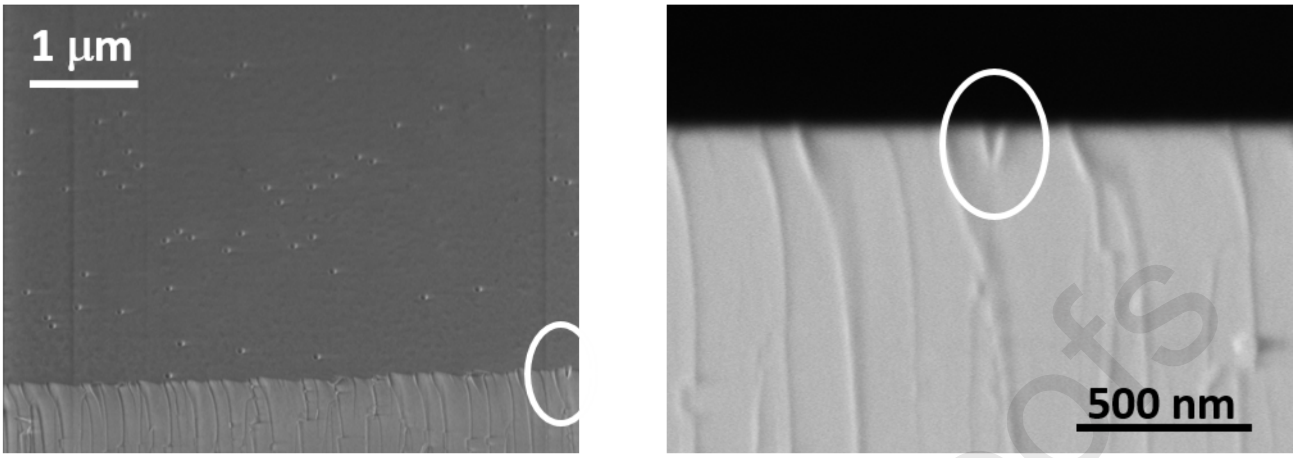

(a) (b)

Figure 1

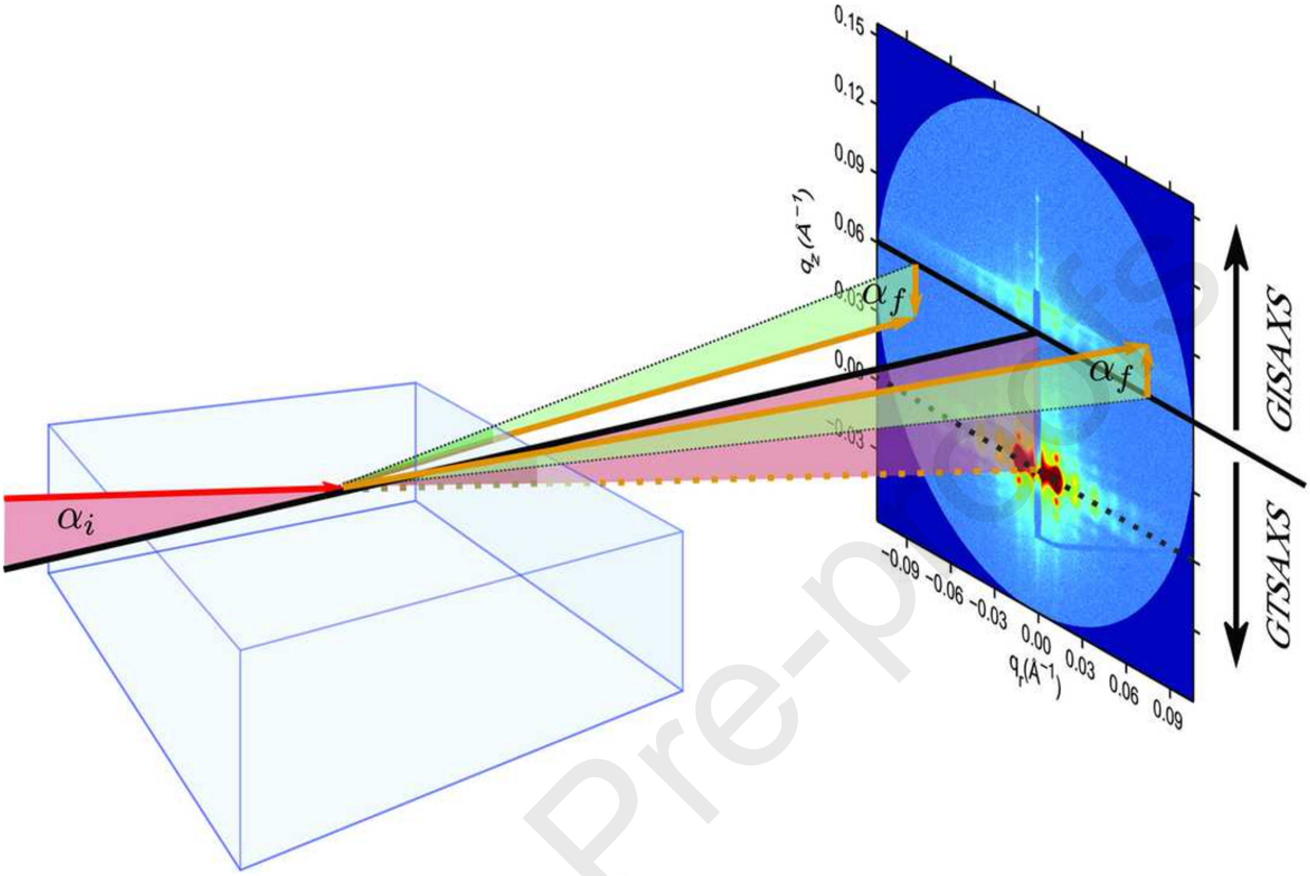
0.15
0.12
0.09
0.06
0.03
0.00
-0.03
q_z (Å^{-1})
α_i
α_f
α_f
-0.09 -0.06 -0.03 0.00 0.03 0.06 0.09
q_r(Å^{-1})
GISAXS
GTSAXS

Figure 2

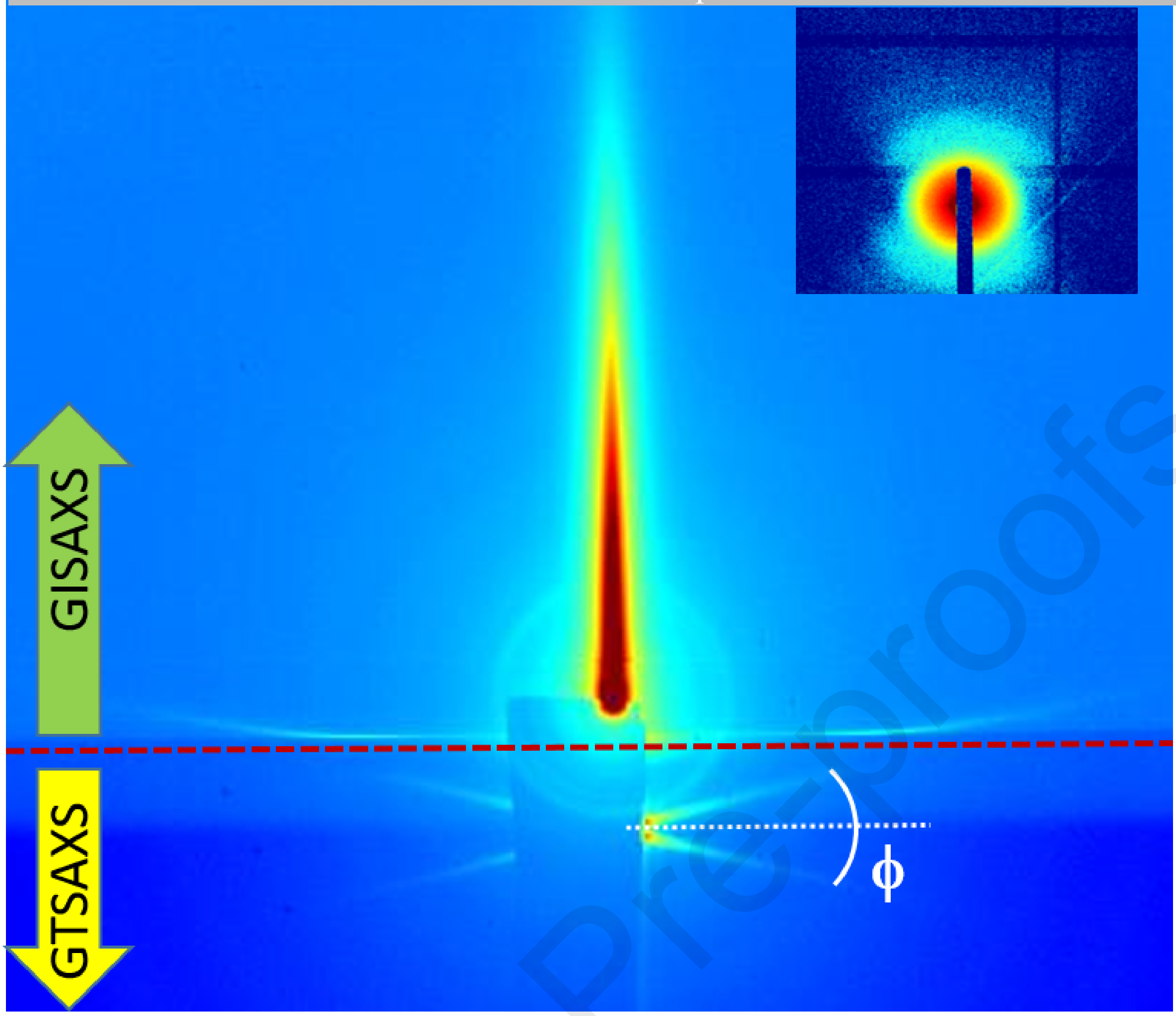

Figure 3

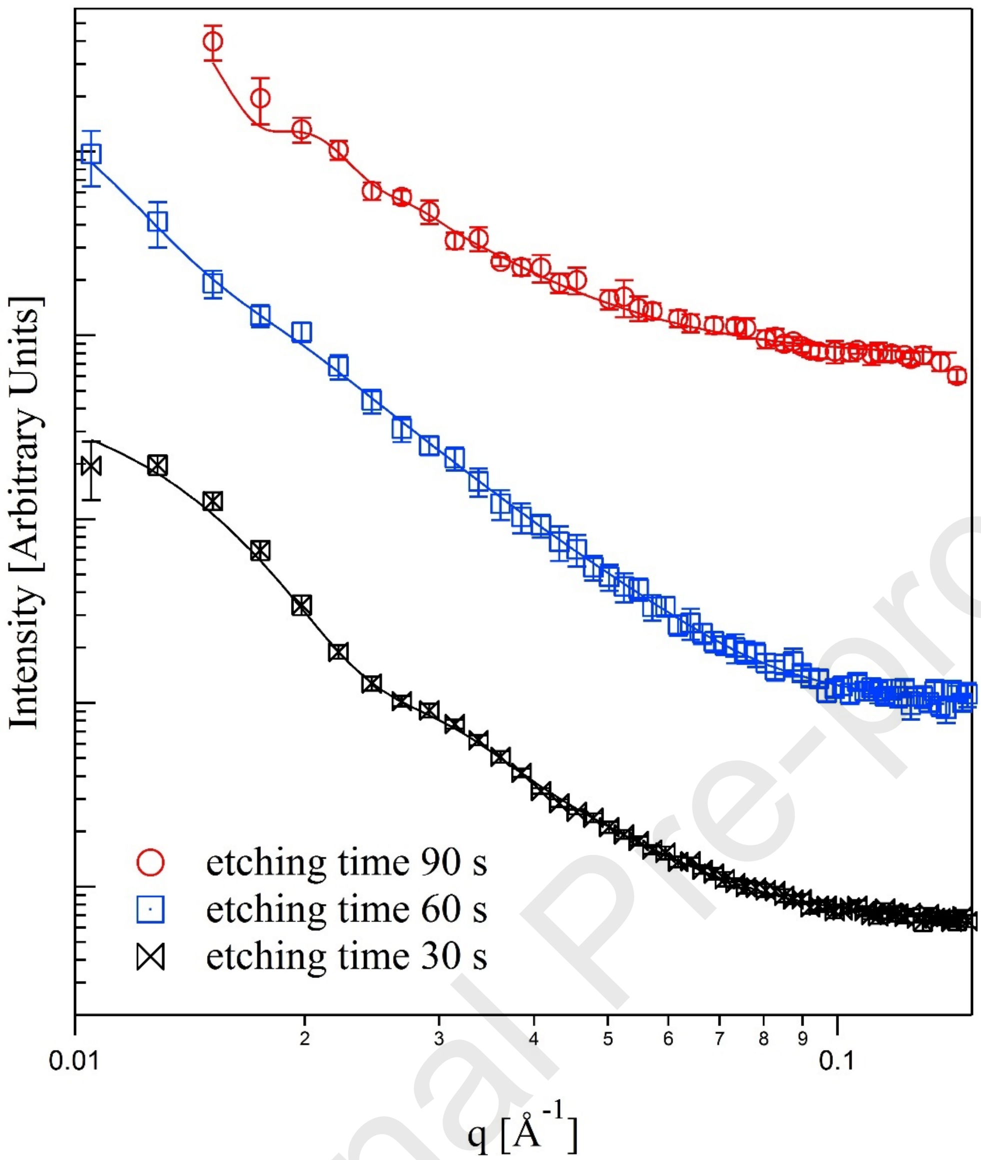
Intensity [Arbitrary Units]
etching time 90 s
etching time 60 s
etching time 30 s
0.01
2
3
4
5
6
7
8
9
0.1
q [Å^-1]

Figure 4

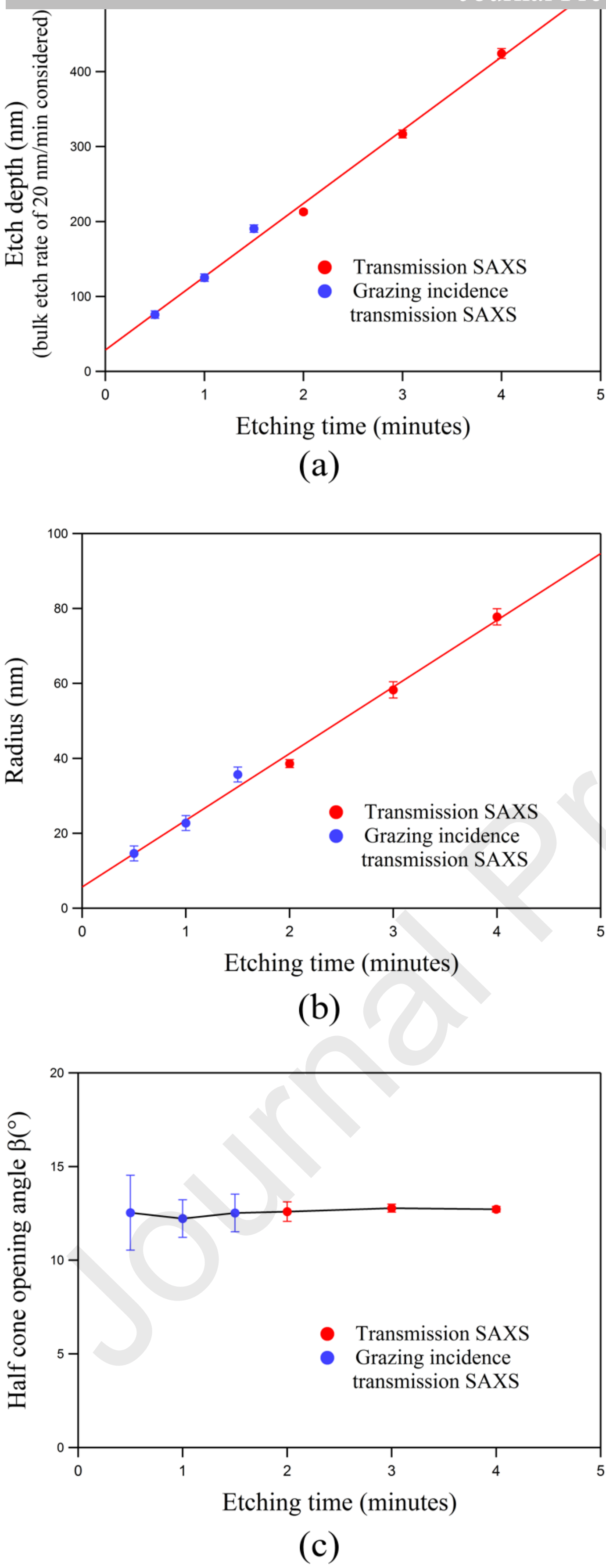
Etch depth (nm)
(bulk etch rate of 20 nm/min considered)
Transmission SAXS
Grazing incidence
transmission SAXS
Etching time (minutes)
(a)
Radius (nm)
Transmission SAXS
Grazing incidence
transmission SAXS
Etching time (minutes)
(b)
Half cone opening angle β(°)
Transmission SAXS
Grazing incidence
transmission SAXS
Etching time (minutes)
(c)

Figure 5